

One-Step Synthesis of Mesoporous Silica Thin Films Containing Available COOH Groups

Ane Escobar,[†] Luis Yate,[†] Marek Grzelczak,^{†,‡,§} Heinz Amenitsch,[§] Sergio E. Moya,[†] Andrea V. Bordoni,^{*,||} and Paula C. Angelomé^{*,||}

[†]CIC biomaGUNE, Paseo de Miramón 182, 20014 Donostia-San Sebastián, Spain

[‡]Ikerbasque, Basque Foundation for Science, 48013 Bilbao, Spain

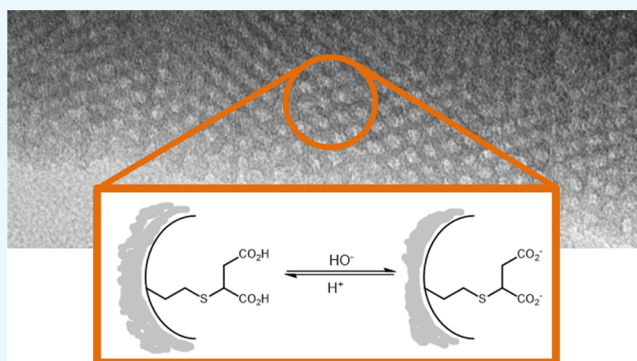
[§]Institute for Inorganic Chemistry, Graz University of Technology, Stremayergasse 9/IV, 8010 Graz, Austria

^{||}Gerencia Química – Centro Atómico Constituyentes, Comisión Nacional de Energía Atómica, CONICET, Avenida General Paz 1499, B1650KNA San Martín, Buenos Aires, Argentina

Supporting Information

ABSTRACT: Inorganic–organic hybrid mesoporous silica thin films with covalently bonded carboxylic acid groups were synthesized in a one-step procedure, using carboxylic-derivatized alkoxy-silanes obtained by photochemical radical thiol-ene addition (PRTEA). The organosilanes were synthesized by clicking mercaptosuccinic or mercaptoacetic thioacids with vinyltrimethoxysilane, using benzophenone as the photo-radical initiator. The films were synthesized by evaporation-induced self-assembly of a sol containing a mixture of tetraethoxysilane and different quantities of the organosilanes, without any further treatment after the PRTEA reaction. Two nonionic surfactants were used as templates to produce different pore sizes. Different aging times were also applied.

Structural characterization with electron microscopy, porosimetry measurements, and small angle X-ray scattering with two-dimensional detection demonstrated the obtention of mesoporous phases whose degree of ordering depended on the amount of added organosilane. The incorporation of the functional silanes was shown by X-ray photoelectron spectroscopy, and the presence of the COOH groups was confirmed by Fourier transform infrared (FTIR). Finally, the availability of the COOH groups for further chemical modification was demonstrated by FTIR by following the changes in the typical carbonyl IR bands during proton exchange and metal complexation. The proposed simple methodology allows obtaining COOH-modified silica thin films in one step, without the need of hard reaction conditions or deprotection steps. Functionalization with carboxyl groups brings a pH-dependent switch-ability to the pore surface that can be used for multifunctional mesoporous materials design.



INTRODUCTION

Oxide-based mesoporous hybrid materials (MHMs) display large surface areas and tunable pore sizes of mesoporous materials, mechanical and thermal stabilities of an inorganic support, and chemical flexibility of organic moieties. In particular, the organic molecules included within the oxide give rise to a complex chemical behavior and provide a means to tailor the pore surface properties, including hydrophobicity and polarity, and catalytic, optical, and electronic characteristics. Thus, MHMs carry the potential for many applications including catalysis, chemical sensing, adsorption, contaminant immobilization, and drug or gene delivery.^{1–3} MHMs in the form of thin films are particularly interesting because they can be easily removed from reaction media and they can be prepared onto a wide variety of surfaces, allowing the easy production of devices.⁴

The incorporation of organic functionalities within porous oxides has attracted increasing attention since the beginning of

the development of mesoporous materials' synthesis. Mainly, two grafting routes are commonly used: postgrafting (postfunctionalization) or co-condensation (one-step approach).^{3,5} In the first case, the functionality is grafted to the material after consolidation of the mesostructure through vapor deposition or solution impregnation. The modification is established through the generation of new bonds between Si–OH or M–OH surface groups and the functionalization agent. The co-condensation method involves the mixing of inorganic precursors with a precursor that bears the organic functionality in the presence of the template; organosilanes are generally used for this approach. Because the mesostructuration and functionalization takes place simultaneously, a portion of the introduced organic groups remains trapped inside the

Received: May 5, 2017

Accepted: June 29, 2017

Published: August 16, 2017

network, thus hindering their accessibility to the medium. Nevertheless, the convenience of the co-condensation method is supported by the reduced number of required processing steps, homogeneous distribution of functional groups within the inorganic network, and reduced pore clogging.

Diverse organic moieties, including mercaptoalkyl, aminoalkyl, phenyl, glycidyl, vinyl, cyanoalkyl, and alkyl groups, just to name a few, have been incorporated onto the pore surface of MHMs, imparting new chemical properties to the pores.^{6,7} Functionalization with carboxylic groups, however, has been less explored when compared with other functional groups. This is due to the lack of suitable commercial reagents and the need for two-step procedures. The functionalization with carboxyl groups brings a pH-dependent switch-ability to the pore surface, whose adsorption capability or catalytic activity can be varied by changing the solution acidity. Needless to mention, there is a possibility of anchoring of biomolecules, such as proteins, antibodies, or folic acid. In addition, COOH can also be used as a ligand for metal complexation in decontamination or detection processes.^{8–10} Nevertheless, several methodologies have been described to achieve the incorporation of the COOH group into silica powders (SBA-15, MCM type, SiO₂ nanoparticles) by co-condensation or postgrafting.¹⁰ These strategies include: modification of a NH₂-functionalized surface with succinic acid, co-condensation or postgrafting with an aqueous solution of carboxyethylsilanetriol, or grafting of an organosilane bearing an ester group that gives rise to free carboxylic moiety after a hydrolysis step.¹⁰ Another possible approach is the use of cyanide to carboxylic methods, wherein the COOH group is obtained after hydrolysis of the –CN group with sulfuric acid using hard experimental conditions: high temperature and long reaction times.¹⁰ Interestingly, the incorporation of COOH groups into mesoporous thin films has been barely reported. Liu et al.¹¹ have shown successful incorporation of carboxylic groups into mesoporous thin films through a co-condensation method, applying the cyanide to carboxylic conversion in a two-step method. However, the lack of literature examples on the direct incorporation of COOH functional groups in mesoporous films is due to the limited commercial availability of carboxyethylsilanetriol sodium salt (available only as a water base solution), being an incompatible precursor in evaporation-induced self-assembly (EISA).¹² In particular, the EISA approach requires low water concentrations to both control the sol–gel reaction and to allow fast evaporation of the sol during film drying. Therefore, there is an obvious lack of reported methods that allowed the incorporation of the COOH functional group into mesoporous thin films using one step approaches.

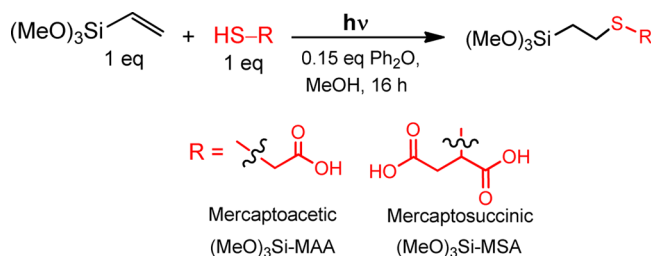
In earlier studies, we have reported the synthesis of organosilanes bearing deprotected carboxylic acids in their structure by photochemical radical thiol–ene addition (PRTEA), which were used without any purification for the modification of mesoporous silica SBA-15 powder by the postfunctionalization approach.⁹ PRTEA is a simple organic reaction, wherein a thiyl radical is added to a double bond connecting two construction blocks through a thioether bond, a click-based modular reaction based on the click-chemistry concept introduced by Sharpless,^{8,13,14} offering simplicity and good conversions. As a consequence, this reaction has generated much interest in the area of materials science in the last few years, both for surface modification and for precursor synthesis.⁸

In this work, we present the direct and unprotected incorporation of COOH moieties in mesoporous hybrid thin films, by a one-step co-condensation approach. The incorporation of the functional group was achieved by reaction between tetraethoxysilane and two different carboxylated alkoxy silanes obtained by PRTEA, using the click reaction product without the need of any purification or deprotection step. The hybrid films were obtained by EISA using two templating agents and different proportions of the modified silanes. Characterization of the obtained films demonstrated that the material displays a mesoporous structure decorated with COOH groups that remain accessible for further chemical reactions in all studied cases.

RESULTS AND DISCUSSION

Two different alkoxy silane-bearing carboxylic moieties, one with a short alkyl chain and one dicarboxylated, were synthesized by PRTEA;⁹ the reaction pathway is presented in Scheme 1.

Scheme 1. Reaction Pathway To Obtain the COOH-Modified Silanes by PRTEA



To prepare the sols, the reaction mixture was used without any purification after completing the click coupling. Different amounts (from 5 up to 20% in molar proportion) of each of the two carboxylated precursors were mixed with tetraethylorthosilicate (TEOS), ethanol, a template, and acidic water. To control the pore-sized nonionic surfactants, F127 and Brij 58 were used as templates. Additionally, the sol aging time was varied in the range of 1–24 h. Samples were named taking into account the template used (F for F127 and B for Brij 58), the carboxylic acid included in the inorganic framework (mercaptosuccinic acid (MSA)-derived silane and mercaptoacetic acid (MAA)-derived silane), its theoretical molar percentage, and the sol's aging time. For example, SiB-MSA 5% 1 h sample refers to a thin film, including the mercaptosuccinic acid function with $x = 0.05$, Brij 58 as the template, and 1 h of aging after the sol preparation. Samples without organic functions ($x = 0$) are denoted as SiF and SiB. See Table S1 for complete information about the studied systems.

All organosilica thin films were obtained by dip coating over glass substrates, taking advantage of the EISA approach.¹² All films presented an excellent optical quality, were well adhered to the substrate and were transparent in the visible region. The films' thicknesses were in the 250–300 nm range, as determined by ellipsometry. This parameter can be easily varied by changing the dip-coating rate.

Structural Characterization. To fully understand the influence of the sol composition on the structural features of oxides, all samples were characterized after template extraction by transmission electron microscopy (TEM) and small-angle X-ray scattering with two dimensional detection (2D-SAXS), the

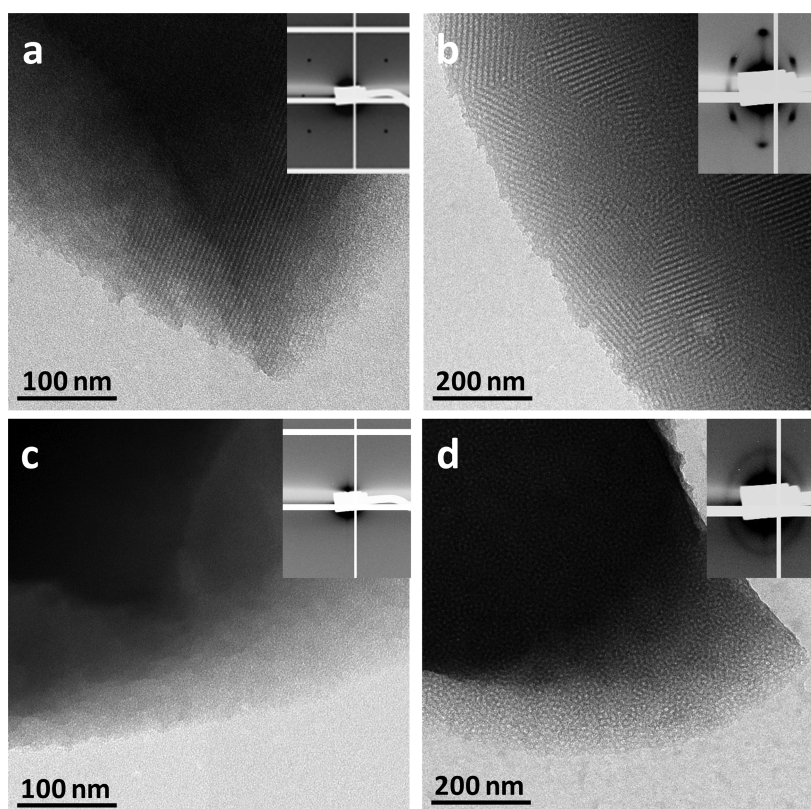


Figure 1. TEM and 2D-SAXS patterns of: (a) SiB-MSA 5% 1 h, (b) SiF-MSA 5% 1 h, (c) SiB-MSA 20% 1 h, and (d) SiF-MSA 20% 1 h thin films.

ideal method to assign the porous structure of mesoporous thin films.¹⁵ Representative images and diffraction patterns are presented in Figures 1 and S1.

In all tested conditions, porous materials were obtained, as can be seen in the TEM images. However, only the oxides with lower concentration of organic silane showed a high degree of order, as observed by both TEM and 2D-SAXS. In fact, for all samples containing 5% of organic moiety, 2D-SAXS patterns can be assigned to a body-centered cubic *Im3m* pore array, oriented with the (110) plane parallel to the substrate. This structure is usually obtained when F127 and Brij 58 are used as templates and is the same structure observed for the samples without organic function.¹⁶ A further increase of the COOH-modified silane incorporation (to 12.5 and 20%) affected the order of the structure. For F127-templated oxides, the 2D-SAXS patterns were ellipses, which correspond to locally ordered (wormlike) arrays of mesopores. Although TEM images demonstrate that Brij 58-templated samples are porous (Figure 1C, as an example), in 2D-SAXS measurements, no pattern was observed.

Our observation agrees with previous studies¹⁷ that show that the presence of organic functions generally limits the organosilane/silane molar ratio in which an ordered structure is obtained, being 20% of the organic function the most usual limit.^{3,6,7} Aging up to 24 h has no effect on the observed behavior, being the high acidity of the initial sol a possible explanation for it.¹¹

Regarding the plane's distances obtained from 2D-SAXS patterns, it is interesting to note that the d_{110} distance (the distance between pores for the cubic structure in the *xy* plane) decreases when the amount of organic function in the films increases, as can be seen as an example for the SiF-MSA case in Table 1.

Table 1. d_{110} Interplanar Distances (in nm) Obtained from 2D-SAXS Patterns for the SiF-MSA System

nominal % of organosilane	aging	
	1 h	24 h
0	14.8	
5	13.3	13.5
12.5	12.6	12.6
20	11.2	11.4

These results could indicate that the diameter of micelles decreases with the increase of concentration of the organic function, resulting in smaller interpore distances. This tendency hints to a concentration-dependent interaction between the templates and the organic moiety, affecting the size of the micelles and ultimately of the pores, which are built using the micelles as templates. A similar tendency has been observed for cetyltrimethylammonium bromide-templated chloropropylsilane-modified silica,¹⁸ but there are no reports for nonionic templates such as the ones presented in this work. We postulate that the interaction of the COOH moieties with the hydrophilic portion of the templates diminishes the hydration of the micelles; thereby, their size decreases.¹⁹ More detailed experiments are being conducted to shed light on this point, also taking into the account the possibility of a decrease in the wall's thicknesses that can lead to the same observed tendency.

Next, to demonstrate the availability of the porous structure, we performed environmental ellipsometric porosimetry (EEP) measurements. This technique is useful to determine accessible porosity and pore sizes in mesoporous thin films because the measurement can be performed directly, without detaching the sample from the substrate.²⁰ Isotherms obtained by EEP, presented in Figure 2, show the typical hysteresis loop of

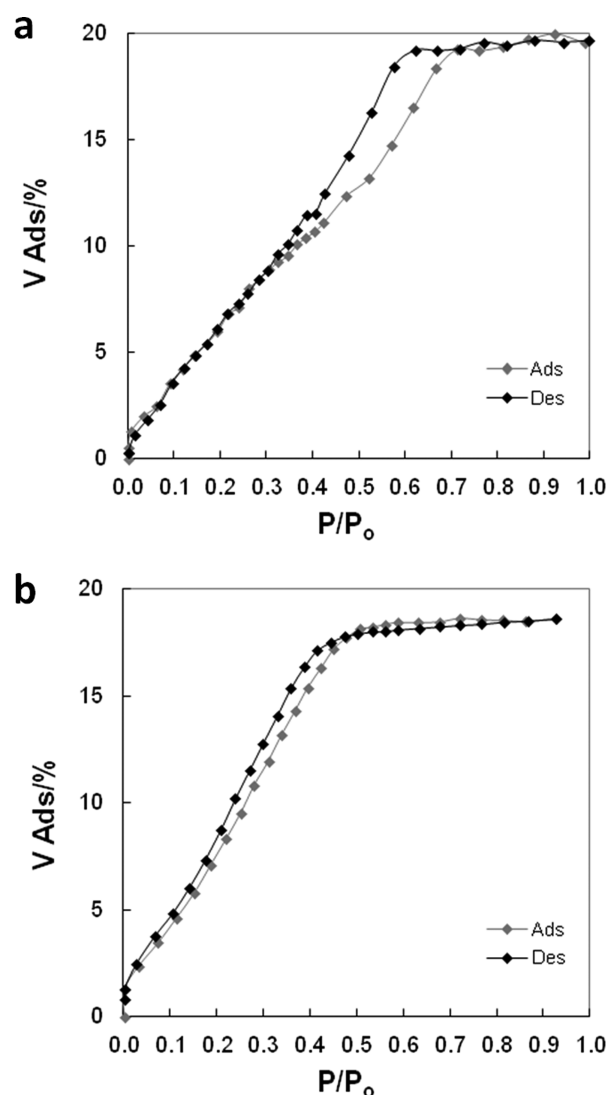


Figure 2. EEP results for (a) SiF-MSA 20% 24 h and (b) SiB-MSA 20% 24 h thin films.

mesoporous materials. From the isotherms' analysis,²⁰ it can be concluded that the films presented an accessible porosity of ~20% and pore diameters of ~4 and ~2 nm for F127 and Brij 58, respectively (Table 2). These values are in agreement with

Table 2. Data Obtained from EEP Measurements

sample	thickness/nm	porosity/%	pore diameter/nm
SiB-MSA 20% 1 h	254	20	2.7
SiB-MSA 20% 24 h	225	19	2.1
SiF-MSA 20% 1 h	285	21	3.9
SiF-MSA 20% 24 h	295	20	4.7

previously obtained results for mesoporous thin films that were treated at moderate temperatures, followed by template extraction using organic solvents. This treatment results in less deformed and interconnected pores, which means that pore sizes are smaller and that films are less porous, compared with the ones that are calcined.^{21,22}

Knowing the final chemical composition and speciation of the organic groups incorporated within the hybrid films is critical for understanding the material's final properties and

potentialities. These results are particularly important for the case of MHMs prepared by the co-condensation methodology because the chance of the organic function's degradation due to thermal treatment is high. X-ray photoelectron spectroscopy (XPS) measurements were performed to determine the chemical composition. As expected, the survey XPS spectra of all hybrid films analyzed showed the presence of Si, O, C, and S, indicating the successful incorporation of carboxylated silanes. Figure 3a shows, as an example, the wide scan spectrum for the SiB-MSA 20% system. All spectra show the Si 2p signal at around 103 eV. From the high-resolution spectra, it can be observed that the samples containing 12.5 and 20% of the carboxylated silanes show the presence of two peaks at 164.2 and 168.6 eV (Figure 3b), whereas the films with 5% only show the peak at 168.6 eV (Figure 3c). The binding energy at ~164.2 eV can be assigned to $-\text{C}-\text{S}-$ ²³ and the one at ~168.6 eV can be associated to the oxidized sulfur species $-\text{C}-\text{SO}_x-\text{C}-$.²³ The oxidation of S was observed in every sample; this observation could be due to the thermal treatment performed in the presence of oxygen.

The XPS survey also gives the content of S and Si in the samples, which can be related to the proportion of carboxylated organosilane incorporated into the films. Because each carboxylated silane molecule contains only one sulfur atom per silicon, the nominal ratio S/Si in sols should be maintained in the films. From atomic percentages obtained from the XPS survey of the films, an experimental ratio between S and Si can be calculated. Results are presented in Table 3. The results show that the increase in the fraction of functionalized silane leads to increase in the final amount of sulfur in the hybrid film. In addition, regardless of the type of sample, the final composition of the functionalizing agent in the film corresponds to ~30% of the nominal composition in the solution. This behavior is presumably due to the degradation of silane during the thermal treatment (200 °C) and/or the template extraction. The effect of sol aging is ruled out as a potential cause of degradation, because the binding energy for the sulfur species and functional silane incorporation in the final material is equivalent for different aging times, indicating that silane remains stable for at least 24 h. This lack of effect is coincident with the conservation of order type, pore sizes, and porosities during aging, as demonstrated previously.

Finally, infrared spectroscopy was used to qualitatively analyze the presence and reactivity of COOH groups. Figure 4 shows, as an example, diffuse reflectance infrared Fourier transform spectroscopy (DRIFT) spectra of selected MSA-modified samples after template extraction, compared to those of unmodified films.

The IR spectrum of SiF-MSA 20% 1 h (Figure 4b) shows the presence of characteristic signals of the carbonyl group, which is absent in the SiF film (Figure 4a): a shoulder band at 1716 cm^{-1} , associated to the carbonyl group's asymmetric mode of the carboxylic acid ($\nu_{\text{C}=\text{O}}$) protonated form, and another band at lower wavenumber (~1578 cm^{-1}).²⁴ Both bands superimpose the band of adsorbed water (scissoring of OH groups). The lower wavenumber band can be attributed to $\text{C}=\text{O}$ stretching of the acidic groups that interact by hydrogen bonding with chemical species on the oxide surface, as Tsai et al. have previously observed by magic angle spinning NMR in powders,²⁵ or to the ionized form of the carboxylic acid.^{26,27} Besides the bands associated to COOH groups, the spectra shows the characteristics bands corresponding to the $\text{O}-\text{Si}-\text{O}$ stretching (TO , TO_2 , and TO_3 modes) of the silica network.²⁸

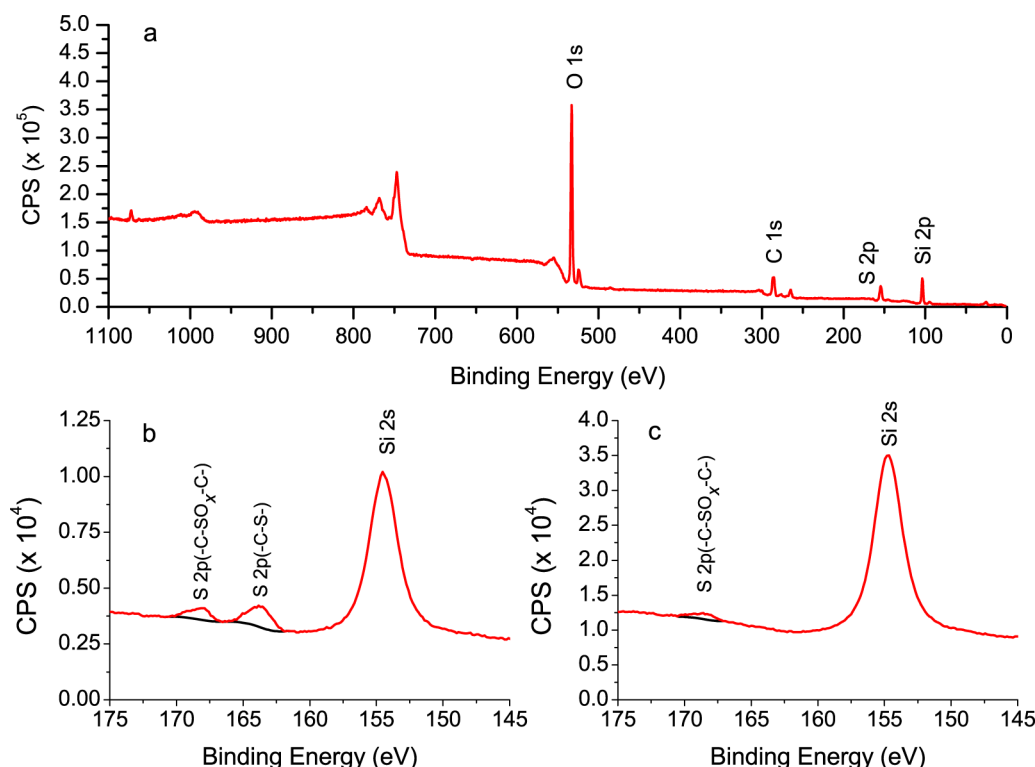


Figure 3. XPS spectra (a) wide scan for SiB-MSA 20% 1 h system; detailed scan in the S and Si region for SiB-MSA 20% 1 h system (b) and SiB-MSA 5% 1 h system (c).

Table 3. Atomic Percentages for S and Si and S/Si Relation Calculated from XPS Spectra of the Different Systems Containing the MSA Moiety

sample	mean S/Si atomic ratio	sample	mean S/Si atomic ratio
SiF-MSA 5% 1 h	0.017 ± 0.005	SiF-MSA 5% 24 h	0.020 ± 0.001
SiF-MSA 12.5% 1 h	0.045 ± 0.003	SiF-MSA 12.5% 24 h	0.048 ± 0.004
SiF-MSA 20% 1 h	0.060 ± 0.004	SiF-MSA 20% 24 h	0.060 ± 0.007
SiB-MSA 5% 1 h	0.010 ± 0.001	SiB-MSA 5% 24 h	0.013 ± 0.002
SiB-MSA 12.5% 1 h	0.050 ± 0.006	SiB-MSA 12.5% 24 h	0.042 ± 0.005
SiB-MSA 20% 1 h	0.060 ± 0.003	SiB-MSA 20% 24 h	0.062 ± 0.005

at 1300–950 and 800 cm^{-1} zones and the Si–OH band at 850 cm^{-1} . Also, the stretching vibration bands corresponding to the aliphatic skeleton of silane and some residue of the template ($\nu_{\text{C-H}}$) are exhibited at 2954, 2927, and 2858 cm^{-1} .

Similar results are obtained for the films containing MAA and/or templated with Brij58 (Figures S2 and S3): COOH related bands are present together with silica skeleton ones. However, it is worth noting that the way the samples are prepared for transmission IR measurements (scratching the film vs preparing the film directly onto a KBr pellet) can affect the relation of the intensities between the two bands attributed to the COOH group probably due to the difference in the films' thicknesses and accessibility.

The shifting and intensity of C=O bands can be used to evaluate the reactivity of COOH/COO[−] groups toward simple reactions, such as acid–base or metal complexation. Note, however, that as the films were obtained by the co-

condensation method, not all carboxylic groups were available on the pore surface. When SiF-MSA 20% film was exposed to HCl vapors (Figure 4c), the intensity of the band located at 1716 cm^{-1} increased with the concomitant disappearance of the band located at $\sim 1578 \text{ cm}^{-1}$, indicating that a fraction of the COOH groups are involved in acid–base equilibrium.²⁴ Immediately after, this film was immersed in 0.4 mM Pb²⁺ aqueous solution. The spectrum (Figure 4d) shows a decrease in the intensity of the band located at 1716 cm^{-1} and the appearance of a distinctive band at 1550 cm^{-1} that is associated with coordinated carboxylic groups.^{24,26,27} Moreover, it can be seen that the 850 cm^{-1} band associated with Si–OH does not suffer any changes after contact with acidic or Pb(II) solutions (Figure 4c,d). This indicates, as expected on the basis of previous results,⁹ that the acidity and ion exchange due to the bare silica matrix are negligible when compared to those due to the COOH groups, under these experimental conditions. Thus, these simple acid–base and coordination experiments show that the included carboxylic groups are available for simple chemical reactions such as proton interchange or Pb(II) ion trapping.

SUMMARY AND CONCLUSIONS

In this work, we have presented the direct incorporation of readily available COOH groups to mesoporous silica thin films by the co-condensation method. Two different carboxylated organosilanes obtained by PRTEA were used, demonstrating the easiness of this reaction and the versatility of the chosen protocol to incorporate organic functions. Moreover, the two different templates (F127 and Brij 58) used in the process showed identical successful results.

Structural characterization demonstrated the generation of mesoporous phases whose degree of ordering depends on the

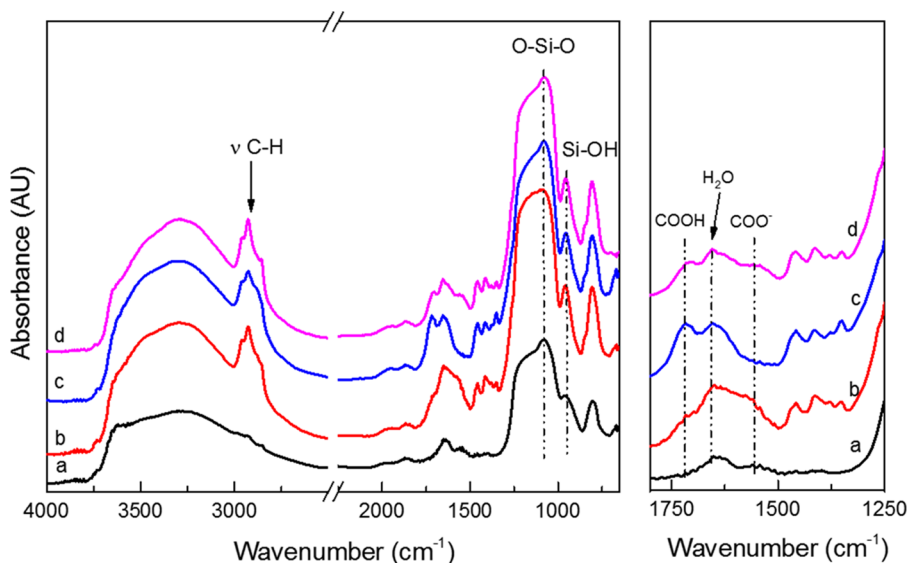


Figure 4. DRIFT spectra of scratched films after extraction: (a) SiF, (b) SiF-MSA 20% 1 h, (c) SiF-MSA 20% 1 h after contact with HCl, and (d) SiF-MSA 20% 1 h after contact with Pb^{2+} . Left: wide spectra. Right: enlargement of the COOH region.

amount of added organosilanes. In particular, low organosilane concentrations give rise to body-centered cubic mesoporous ordering, whereas higher concentrations give rise to locally ordered structures. The incorporation of functional silanes was clearly demonstrated by XPS, showing that around 30% of the nominal organosilane concentration is incorporated within the films.

The presence of COOH groups on the pore surface was confirmed by infrared spectroscopy alongside with its availability for further chemical modification. Clear changes in the typical carbonyl signals during proton interchange and metal complexation experiments were observed, indicating that chemical reactions can be performed on the modified mesoporous structure.

The proposed simple methodology allows the synthesis of COOH-modified silica thin films in one step, without the need of hard reaction conditions or deprotection steps. Moreover, as the material is obtained as a thin film, it can be easily incorporated in reaction media and/or integrated into devices. As COOH groups are expected to serve as binding sites for more complex molecules, such as proteins, enzymes, or ions, the presented results pave the way toward applications of such COOH-modified films, for example, as sensors or drug-delivery devices.

EXPERIMENTAL SECTION

Materials. TEOS (98%), vinyltrimethoxysilane (VTMS, 98%), mercaptoacetic acid (MAA, 97%), 2-mercaptosuccinic acid (MSA, 97%), benzophenone (Ph_2CO , 99%), Brij 58, and Pluronic F127 were purchased from Sigma-Aldrich and used as received. Hydrochloric acid (37%), $\text{Pb}(\text{NO}_3)_2$, and methanol were purchased from Merck. Methanol, pure grade ethanol, and Milli-Q water were used as solvents. Methanol was dried over activated MS-3 Å before use.

Synthesis of Carboxylic Trialkoxysilane Precursors. 2-((2-(Trimethoxysilyl)ethyl)thio)succinic acid ($(\text{MeO})_3\text{Si-MSA}$) and 2-((2-(trimethoxysilyl)ethyl)thio)acetic acid ($(\text{MeO})_3\text{Si-MAA}$) were prepared, as previously reported.⁹ Briefly, 1 equiv of VTMS was added to a vial containing methanol solution of the desired amount of MSA or MAA

(chosen according to the desired proportion of organic function in the final material, see below) and 0.15 equiv of Ph_2CO as the photoinitiator (Scheme 1). Reaction solutions were then irradiated under gentle stirring for 16 h, using a 15 W, 18" long black-light lamp ($\lambda_{\text{max}} = 352 \text{ nm}$). The precursor's reaction mixture was used without any further treatment in the preparation of the sols.

Preparation of Hybrid Mesoporous Thin Films. Hybrid sols were prepared in three steps: (1) TEOS, ethanol, and the template (Brij 58 or F127) were mixed; (2) the reaction mixture of thio-ene addition was added drop wise under stirring; and (3) HCl solution was added drop wise under stirring. The chosen order allows the correct co-condensation reaction between the two silanes. The theoretical molar proportions of the sols were $\text{TEOS/Si-R/template/HCl/EtOH/H}_2\text{O} = 1 - x:x:s:0.28:24:5.2$, with $0 \leq x \leq 0.2$, R = MSA or MAA, and $s = 0.005$ for F127 or $s = 0.05$ for Brij 58. After its preparation, the sol was aged for different times in the 1–24 h range.

Hybrid mesoporous $\text{Si}_{1-x}(\text{SiR})_x\text{O}_2$ films were synthesized by dip coating, taking advantage of the EISA approach.¹² A withdrawal speed of 3 mm s^{-1} was used to deposit the films onto glass slides. Immediately after synthesis, the films were placed in a humidity-controlled chamber at 50% relative humidity (obtained with a saturated $\text{Ca}(\text{NO}_3)_2$ solution in water) and kept there for 24 h. Afterward, they were submitted to a gentle thermal treatment: 24 h at 60°C , 24 h at 130°C , and 2 h at 200°C . Finally, the template was extracted by immersing the films for 2 days in pure grade ethanol.

Characterization. 2D-SAXS patterns were obtained at the Austrian SAXS beamline at the Elettra synchrotron (Trieste, Italy), using a 1.54 Å (8 keV) incidence X-ray beam.²⁹ The sample was placed at 82.88 cm from a pixel detector (Pilatus 1M) on a rotation stage, which allowed to set the glancing angle between the incident radiation and the sample to 3° . The samples were prepared onto coverslips to allow measurements in Laue geometry. The angular scale of the detector was calibrated with Ag-behenate as the reference pattern.

Pores were visualized by TEM using a JEOL JEM-1400PLUS microscope equipped with a Gatan US1000 CCD camera.

Samples were prepared by dropping pure ethanol on carbon-coated copper grids and depositing the powder obtained after scratching the films.

The atomic composition of the films was determined by XPS, with a SPECS Sage HR 100 spectrometer equipped with a 100 mm mean radius PHOIBOS analyzer and a nonmonochromatic X-ray source (Mg K α line of 1253.6 eV energy and 250 W), placed perpendicular to the analyzer axis and calibrated using the 3d_{5/2} line of Ag, with a full width at half maximum of 1.1 eV. The selected resolution for high resolution spectra was 15 eV of pass energy and 0.15 eV per step. All measurements were made in an ultrahigh vacuum chamber at a pressure of around 8×10^{-8} mbar. An electron flood gun was used to neutralize for charging. Measurements were conducted directly on the films, which were previously washed with absolute ethanol and cut into samples of 1 cm \times 1 cm. The analysis of spectra was done with CasaXPS 2.3.15dev87 software. Satellite removal and Shirley background subtraction were applied, the binding energies were calibrated assigning to the C 1s C–C peak 285 eV, and peaks were fitted with Gaussian–Lorentzian line shapes to determine the atomic percentages of elements present in the films. To calculate the atomic ratio between sulfur and silicon, three different films of each system were measured.

Ellipsometric and EEP measurements were performed in a SOPRA GESSA ellipsometer, using samples previously washed with absolute ethanol and dried. Film thickness and refractive index values were obtained from the ellipsometric parameters Ψ and Δ under dry air flux containing variable water vapor pressure P ; P/P_0 was varied from 0 to 1 (P_0 being the saturation water vapor pressure at 25 °C). Water volume adsorbed at each P/P_0 value was determined by modeling the obtained refractive index according to a three-component (water–air–oxide) Bruggeman effective medium approximation. Adsorption–desorption isotherms were obtained by plotting the water volume adsorbed by the porous film at each P/P_0 . The pore size distribution was obtained from the isotherms using the Kelvin equation, taking into account the water contact angle in the film.²⁰ Water contact angles required for such calculations were determined using a Ramé–Hart 190 CA equipment.

FTIR spectroscopy and DRIFT measurements were performed in a Nicolet Magna 560 instrument, equipped with a liquid N₂-cooled MCT-A detector. For transmission measurements, a drop of each sol was deposited onto a KBr pellet and treated in the same way as the thin films. Measurements were made at different stages of the thermal treatment. DRIFT measurements were performed by depositing scratched films onto a KBr-filled sample holder. To observe the speciation and accessibility of the COOH group in the inorganic network, the films were dried for 10 min in a 130 °C oven and immediately after scratched; the spectrum was taken immediately to minimize the water adsorption from the environment. In the case of acidic treatment, the films were set for 10 min in a chamber saturated with HCl vapor. Then, the films were dried and scratched in a similar way, as with the untreated films. For metal coordination studies, the films were put in contact with a 0.4 mM Pb²⁺ aqueous solution for 5 min, washed with water and ethanol, dried, and then scratched.

■ ASSOCIATED CONTENT

● Supporting Information

The Supporting Information is available free of charge on the ACS Publications website at DOI: 10.1021/acsomega.7b00560.

Complete set of samples' list; TEM images, 2D-SAXS patterns, and IR spectra of complementary samples (PDF)

■ AUTHOR INFORMATION

Corresponding Authors

*E-mail: abordoni@cnea.gov.ar (A.V.B.).

*E-mail: angelome@cnea.gov.ar (P.C.A.).

ORCID

Marek Grzelczak: 0000-0002-3458-8450

Sergio E. Moya: 0000-0002-7174-1960

Andrea V. Bordoni: 0000-0003-1235-6170

Paula C. Angelomé: 0000-0002-4402-5045

Notes

The authors declare no competing financial interest.

■ ACKNOWLEDGMENTS

This work has been funded by CONICET (PIP 00044CO), ANPCyT (PICT 2012-0111, PICT 2013-1303, and PICT 2015-0351), and European Union's Horizon 2020 Programme under the Marie Skłodowska-Curie grant agreement No. 645686 (HYMADE). The authors acknowledge the CERIC-ERIC consortium for the access to experimental facilities at the Elettra synchrotron, Trieste and the financial support.

■ REFERENCES

- (1) Sánchez, C.; Boissiere, C.; Cassaignon, S.; Chaneac, C.; Durupthy, O.; Faustini, M.; Grosso, D.; Laberty-Robert, C.; Nicole, L.; Portehault, D.; Ribot, F.; Rozes, L.; Sassoey, C. Molecular Engineering of Functional Inorganic and Hybrid Materials. *Chem. Mater.* **2014**, *26*, 221–238.
- (2) Soler-Illia, G. J. A. A.; Innocenzi, P. Mesoporous hybrid thin films: The physics and chemistry beneath. *Chem. – Eur. J.* **2006**, *12*, 4478–4494.
- (3) Sánchez, C.; Boissiere, C.; Grosso, D.; Laberty, C.; Nicole, L. Design, Synthesis, and Properties of Inorganic and Hybrid Thin Films Having Periodically Organized Nanoporosity. *Chem. Mater.* **2008**, *20*, 682–737.
- (4) Innocenzi, P.; Malfatti, L. Mesoporous thin films: properties and applications. *Chem. Soc. Rev.* **2013**, *42*, 4198–4216.
- (5) Nicole, L.; Boissiere, C.; Grosso, D.; Quach, A.; Sanchez, C. Mesoporous hybrid organic-inorganic thin films. *J. Mater. Chem.* **2005**, *15*, 3598–3627.
- (6) Cagnol, F.; Grosso, D.; Sanchez, C. A general one-pot process leading to highly functionalised ordered mesoporous silica films. *Chem. Commun.* **2004**, *15*, 1742–1743.
- (7) Soler-Illia, G. J. A. A.; Azzaroni, O. Multifunctional hybrids by combining ordered mesoporous materials and macromolecular building blocks. *Chem. Soc. Rev.* **2011**, *40*, 1107–1150.
- (8) Bordoni, A.; Lombardo, M. V.; Wolosiuk, A. Photochemical radical thiol-ene click-based methodologies for silica and transition metal oxides materials chemical modification: a mini-review. *RSC Adv.* **2016**, *6*, 77410–77426.
- (9) Bordoni, A. V.; Lombardo, M. V.; Regazzoni, A. E.; Soler-Illia, G. J. A. A.; Wolosiuk, A. Simple thiol-ene click chemistry modification of SBA-15 silica pores with carboxylic acids. *J. Colloid Interface Sci.* **2015**, *450*, 316–324.
- (10) Han, L.; Terasaki, O.; Che, S. Carboxylic group functionalized ordered mesoporous silicas. *J. Mater. Chem.* **2011**, *21*, 11033–11039.
- (11) Liu, N.; Assink, R. A.; Brinker, C. J. Synthesis and characterization of highly ordered mesoporous thin films with -COOH terminated pore surfaces. *Chem. Commun.* **2003**, *9*, 370–371.
- (12) Brinker, C. J.; Lu, Y.; Sellinger, A.; Fan, H. Evaporation-Induced Self-Assembly: Nanostructures Made Easy. *Adv. Mater.* **1999**, *11*, 579–585.

- (13) Kolb, H. C.; Finn, M. G.; Sharpless, K. B. Click Chemistry: Diverse Chemical Function from a Few Good Reactions. *Angew. Chem., Int. Ed.* **2001**, *40*, 2004–2021.
- (14) Espeel, P.; Du Prez, F. E. “Click”-inspired chemistry in macromolecular science: Matching recent progress and user expectations. *Macromolecules* **2015**, *48*, 2–14.
- (15) Soler-Illia, G. J. A. A.; Angelomé, P. C.; Fuertes, M. C.; Grosso, D.; Boissiere, C. Critical aspects in the production of periodically ordered mesoporous titania thin films. *Nanoscale* **2012**, *4*, 2549–2566.
- (16) Angelomé, P. C.; Fuertes, M. C.; Soler-Illia, G. J. A. A. Multifunctional, Multilayer, Multiscale: Integrative synthesis of complex macro and mesoporous thin films with spatial separation of porosity and function. *Adv. Mater.* **2006**, *18*, 2397–2402.
- (17) Nicole, L.; Boissiere, C.; Grosso, D.; Hesemann, P.; Moreau, J.; Sanchez, C. Advanced selective optical sensors based on periodically organized mesoporous hybrid silica thin films. *Chem. Commun.* **2004**, 2312–2313.
- (18) Gibaud, A.; Bardeau, J. F.; Dutreilh-Colas, M.; Bellour, M.; Balasubramanian, V. V.; Robert, A.; Mehdi, A.; Reye, C.; Corriu, R. J. Influence of functional organic groups on the structure of CTAB templated organosilica thin films. *J. Mater. Chem.* **2004**, *14*, 1854–1860.
- (19) Doshi, D. A.; Gibaud, A.; Liu, N.; Sturmayer, D.; Malanoski, A. P.; Dunphy, D. R.; Chen, H.; Narayanan, S.; MacPhee, A.; Wang, J.; Reed, S. T.; Hurd, A. J.; van Swol, F.; Brinker, C. J. In-Situ X-ray Scattering Study of Continuous Silica-Surfactant Self-Assembly during Steady-State Dip Coating. *J. Phys. Chem. B* **2003**, *107*, 7683–7688.
- (20) Boissiere, C.; Grosso, D.; Lepoutre, S.; Nicole, L.; Bruneau, A. B.; Sanchez, C. Porosity and Mechanical Properties of Mesoporous Thin Films Assessed by Environmental Ellipsometric Porosimetry. *Langmuir* **2005**, *21*, 12362–12371.
- (21) Violi, I. L.; Perez, M. D.; Fuertes, M. C.; Soler-Illia, G. J. A. A. Highly ordered, accessible and nanocrystalline mesoporous TiO₂ thin films on transparent conductive substrates. *ACS Appl. Mater. Interfaces* **2012**, *4*, 4320–4330.
- (22) Twaiq, F.; Nasser, M. S.; Onaizi, S. A. Effect of the degree of template removal from mesoporous silicate materials on their adsorption of heavy oil from aqueous solution. *Front. Chem. Sci. Eng.* **2014**, *8*, 488–497.
- (23) Qiao, Y.; Ma, M.; Liu, Y.; Li, S.; Lu, Z.; Yue, H.; Dong, H.; Cao, Z.; Yin, Y.; Yang, S. First-principles and experimental study of nitrogen/sulfur co-doped carbon nanosheets as anodes for rechargeable sodium ion batteries. *J. Mater. Chem. A* **2016**, *4*, 15565–15574.
- (24) Fitch, A.; Dragan, S. Infrared Spectroscopy Determination of Lead Binding to Ethylenediaminetetraacetic Acid. *J. Chem. Educ.* **1998**, *75*, 1018.
- (25) Tsai, H.-H. G.; Jheng, G.-L.; Kao, H.-M. Direct Evidence for Interactions between Acidic Functional Groups and Silanols in Cubic Mesoporous Organosilicas. *J. Am. Chem. Soc.* **2008**, *130*, 11566–11567.
- (26) Silverstein, R. M.; Bassler, G. C.; Morrill, T. C. *Spectrometric Identification of Organic Compounds*, 5th ed.; John Wiley and Sons, Inc., 1991.
- (27) Socrates, G. *Infrared and Raman Characteristic Group Frequencies: Tables and Charts*; John Wiley and Sons, 2004.
- (28) Innocenzi, P. Infrared spectroscopy of sol-gel derived silica-based films: a spectra-microstructure overview. *J. Non-Cryst. Solids* **2003**, *316*, 309–319.
- (29) Amenitsch, H.; Bernstorff, S.; Kriechbaum, M.; Lombardo, D.; Mio, H.; Rappolt, M.; Laggner, P. Performance and First Results of the ELETTRA High-Flux Beamline for Small-Angle X-ray Scattering. *J. Appl. Crystallogr.* **1997**, *30*, 872–876.